The control of protein arginine phosphorylation facilitates proteostasis by an AAA+ chaperone protease system

Regina Alver[1,2,4], Ingo Hantke[2,4], Fabián A. Cornejo[1], Katrin Gunka[2], Sebastian Rämisch[1], Noël Molière[2], Emmanuelle Charpentier[1,3] & Kürşad Turgay[1,2*]

[1]*Max Planck Unit for the Science of Pathogens, Berlin, Germany*
[2]*Institut für Mikrobiologie, Leibniz-Universität Hannover, Hannover, Germany*
[3]*Institut für Biologie, Humboldt-Universität zu Berlin, Berlin, Germany*
[4]The authors contributed equally to this work.

[*]for correspondence: Kürşad Turgay, Max Planck Unit for the Science of Pathogens, Charitéplatz 1, 10117 Berlin, Germany; e-mail turgay@mpusp.mpg.de

Running title: protein arginine phosphorylation in protein homeostasis

Keywords: Stress response, protein arginine phosphorylation, protein homeostasis, chaperones, AAA+ proteins, adaptor proteins, McsB kinase, YwlE phosphatase, ClpCP

Abstract

We could demonstrate that the AAA+ unfoldase ClpC together with the protein arginine kinase and adaptor protein McsB, its activator McsA and the phosphatase YwlE form a unique chaperone system. Here, the McsA-activated McsB phosphorylates and targets aggregated substrate proteins for extraction and unfolding by ClpC. Sub-stoichiometric amounts of the YwlE phosphatase enhanced the ClpC/McsB/McsA mediated disaggregation and facilitated the de-phosphorylation of the arginine-phosphorylated substrate protein extruded by ClpC, allowing its subsequent refolding. Interestingly, the successfully refolded protein escaped degradation by the loosely associated ClpP protease. This unique chaperone system is thereby able to disaggregate and refold aggregated proteins but can also remove severely damaged protein aggregates by degradation.

Introduction

Molecular chaperone systems monitor and maintain cellular protein homeostasis. These include chaperone systems such as the Hsp70 & 40 or the Hsp60 system, which can refold and repair misfolded proteins. In many bacteria and yeast, AAA+ unfoldases such as Hsp104 (ClpB) form with DnaK (Hsp70) a bi-chaperone system that can disaggregate and refold and thereby remove and repair already aggregated protein species. The proteolytic arm of the bacterial protein quality control system includes AAA+ protease complexes, consisting of AAA+ unfoldases, such as ClpC, associated with a compartmentalized ClpP protease complex, allowing to degrade and thereby remove more severely damaged and possibly toxic protein aggregate species. The substrate recognition and selection by these AAA+ unfoldases often depend on adaptor proteins that can recognize and target substrate proteins. Notably, adaptor proteins, controlling the activity and stability of key transcription factors, allow AAA+ protease complexes such as ClpCP, ClpAP or ClpXP to be involved in regulatory proteolysis (*1–6*).

The ClpCP AAA+ protease complex of *B. subtilis* is directly involved in general and regulatory proteolysis, including heat stress response and removing subcellular protein aggregates (*7–11*). The substrate recognition and activation of ClpC depends on adaptor proteins, MecA, its paralog YpbH and the protein kinase McsB. The role of YpbH is not well understood (*12*, *13*), MecA is involved in controlling competence development (*14*), and McsB is known for its role in controlling CtsR-mediated heat shock response (*15*).

The protein kinase activity of the McsB adaptor protein catalyzes the formation of a phospho-arginine protein modification with a high-energy phosphoramidate bond (*16*). McsB autophosphorylates itself, and in the presence of McsA, the arginine kinase activity is further induced, resulting in increased autophosphorylation and enhanced phosphorylation of McsA, ClpC and substrate proteins such as the repressor CtsR. YwlE is the cognate phospho-arginine phosphatase, which can counteract the McsB kinase activity, thereby controlling the extent of this protein modification in *B. subtilis* (*15–22*).

53 McsB, like the other adaptor proteins, can interact with the NTD of ClpC, thereby targeting
54 substrate protein for ClpCP degradation. This activity can occur independently of the arginine
55 phosphorylation of the substrate (*15*, *23*, *24*). However, a clear link was observed between the
56 kinase activity of McsB, ClpC activation and its ability to target substrate proteins (*15*, *17*, *19*,
57 *22*). Recently, an additional mechanism of substrate targeting to ClpC was described, where
58 protein arginine phosphorylation by McsB functions as a degron to mark an unfolded substrate
59 protein for direct recognition by the N-terminal domain of ClpC, leading to subsequent
60 degradation by ClpCP (*22*, *25*).
61 A very pleiotropic influence of protein arginine phosphorylation in *B. subtilis* physiology and
62 regulatory pathways, which includes *B. subtilis* spore germination (*26*, *27*), was observed in a
63 *ywlE* mutant (*17*, *20*). However, the role and function of this protein modification system and
64 the interplay of the respective kinase and phosphatase with the ClpC chaperone system in
65 cellular protein homeostasis, is not well understood.

66 ## Results

67 **McsB is the main ClpC adaptor protein allowing the *in vivo* removal of subcellular protein**
68 **aggregates.**

69 To identify which of the adaptor proteins is supporting the role of ClpC in protein homeostasis,
70 we constructed a triple adaptor mutant strain (TAM) lacking the genes for the three known
71 ClpC adaptor proteins (Δ*mecA*Δ*ypbH*Δ*mcsB*). This TAM strain was impaired in
72 thermoresistance and in its ability to develop thermotolerance (Fig 1A & S1A). We ectopically
73 introduced and expressed each single adaptor protein gene in this TAM strain (Fig 1BC Fig
74 S1BD) and observed that only the expression of *mcsB*, and not *ypbH* or *mecA*, was able to
75 confer thermoresistance and thermotolerance at a level comparable to the wild type strain of *B.*
76 *subtilis* (Fig 1B, Fig S1BC). In addition, after a 90 min recovery at 37 °C, only the expression
77 of *mcsB* resulted in the complete removal of heat-induced sub-cellular protein aggregates,
78 marked by the YocM-mCherry reporter (*9*), (Fig 1C, FigS1E). Furthermore, McsB-GFP co-

localized *in vivo* with these subcellular protein aggregates (Fig S1FG), as observed for its substrate CtsR after a heat shock (*28*).

These experiments strongly suggest that McsB is the ClpC adaptor protein necessary and sufficient for thermoresistance and thermotolerance development and to target subcellular protein aggregates for ClpC-dependent removal (*9*) (Fig 1 & Fig S1).

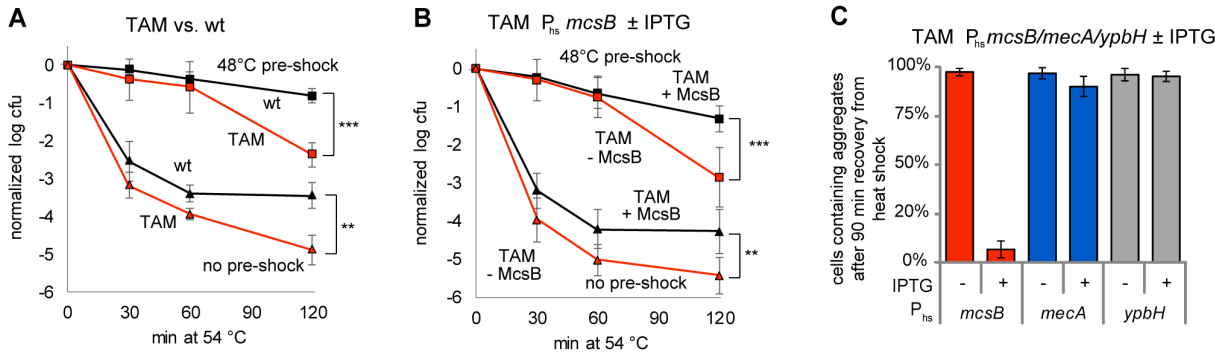

Figure 1 Role of the adaptor protein McsB in protein homeostasis

A) Thermotolerance (squares: with pre-shock) and Thermoresistance (triangles: without pre-shock) experiments analyzing *B. subtilis* Δ*mecA*Δ*ypbH*Δ*mcsB* ('TAM', BIH737, red) and wild-type (black) strains. **B**) *B. subtilis* TAM P_{hs} *mcsB* strain (BIH739), with (black) and without IPTG (red), were examined in a thermotolerance (squares: with pre-shock at 48 °C) and thermoresistance (triangles: no pre-shock) experiment. Log_{10}-values of viable cell count were normalized, and three biological replicates were used to calculate standard deviations (error bars) with significant differences indicated (*: $p<0.05$, **: $p<0.01$, ***: $p<0.001$). **C**) Subcellular protein aggregates during recovery after heat stress *in vivo*. The ratio of cells containing protein aggregates marked by YocM-mCherry of complemented *B. subtilis* TAM strains (TAM P_{hs} *mscsB* (BIH739), TAM P_{hs} *mecA* (BIH740), TAM P_{hs} *ypbH* (BIH741), which were heat shocked for 30 min at 50°C and recovered for 90 min at 37°C, was determined based on three biological replicates including three technical replicates of 50 – 100 cells. Samples were taken at indicated time points for analysis by fluorescence microscopy (see also Fig S1D).

McsA-activated McsB kinase facilitates ClpC disaggregation but interferes with the subsequent *in vitro* refolding of aggregated Mdh

We used heat-aggregated malate dehydrogenase (Mdh) as a model substrate to reconstitute and assess the disaggregation and refolding activities of this chaperone system *in vitro* (*13*, *29*, *30*). In control experiments, we confirmed that the enzyme activity of folded Mdh was not significantly diminished by the active McsB kinase (Fig S1J). We could demonstrate that the well-characterized *E. coli* ClpB, DnaK, DnaJ and GrpE (ClpB/KJE) chaperone system (*29*) fully dissolved the Mdh protein aggregate and facilitated the recovery of 30% of enzyme

activity (Fig S1H). Moreover, as previously observed, the ClpC/MecA chaperone system facilitated a slower disaggregation with a less effective refolding of about 15% (*13*) (Fig S1H). Adding McsB, McsA & ClpC to the heat-aggregated Mdh resulted in an apparent initial complex formation, but the subsequent disaggregation of the substrate protein was lower than observed for ClpB/KJE (Fig S1H, left panel), and only very little refolding (about 5%) could be observed (Fig S1H, right panel).

In supernatant/pellet experiments analyzed by SDS-PAGE, only the solubilization of aggregated Mdh by ClpB/KJE could be detected (Fig S1I). With an immuno-blot utilizing an antibody generated to detect protein arginine phosphorylation (*31*), we observed that most of the arginine phosphorylated proteins could be detected after 15 min, mostly in the soluble fraction (Fig S1I). This coincides with the initial disaggregation complex of ClpC/McsB/McsA appeared to become stabilized and active, as observed by light scattering (Fig S1H, Fig S1I). The relatively low refolding activity by ClpC, McsB and McsA (Fig S1H) might be explained by the unhinged McsA-induced kinase activity of McsB (Fig S1I), whereby the protein arginine phosphorylation of the substrate protein could interfere with its successful refolding.

To further assess the influence of the arginine phosphorylation by McsA and McsB on refolding, we utilized the kinase-inactive McsB C167S variant (*15*, *19*), which could activate *in vitro* the ClpC ATPase activity to about 50 % of McsB-mediated activation (Fig S2C).

McsB C167S could facilitate the ClpC mediated disaggregation reaction *in vitro*, albeit with a slower kinetic, but reaching a similar yield after 120 min (Fig S2E). Importantly, with McsB C167S we observed *in vitro* a significantly increased recovery of Mdh activity to about 20% of the initial activity compared to the 5% of McsB with McsA (Fig. S2E) or the 15% in the presence of MecA (Fig S1H).

While no disaggregation activity was detected *in vivo* in the absence of McsB, we observed partial disaggregation activity at about 25% when complementing a Δ*mcsB B. subtilis* strain with the McsB C167S variant compared to wild-type McsB (Fig S2B). The kinase-inactive

133 *mcsB* C167S mutant strain was impaired by about one order of magnitude in developing
134 thermotolerance or thermoresistance (Fig S2A). We observed a comparable *in vivo* co-
135 localization to subcellular protein aggregates by the kinase-inactive McsB C167S-GFP and the
136 McsB-GFP fusion proteins, suggesting that McsB can recognize subcellular protein aggregates
137 independently of its kinase activity (Fig S2D).
138 In summary, the kinase-inactive McsB C167S variant behaved to a certain extent like a ClpC
139 adaptor protein and allowed, in contrast to kinase-active McsB, a significant refolding of the
140 unfolded substrate protein (Fig S2E & S2F), suggesting that active substrate phosphorylation
141 by McsB might interfere with the subsequent refolding reaction.

142 **The presence of sub-stoichiometric amounts of the YwlE phosphatase facilitates McsB**
143 **kinase-mediated *in vitro* disaggregation and refolding by ClpC**

144 These experiments suggested that controlling the protein arginine phosphorylation state might
145 be very important for the disaggregation and refolding activity of the McsB/McsA/ClpC
146 chaperone complex (*17*, *20*). Previous *in vitro* experiments demonstrated that equimolar
147 amounts of YwlE can inhibit the McsB and McsA-mediated activation of ClpC (*15*). However,
148 when we lowered the YwlE concentration, we observed that at sub-stoichiometric levels of
149 YwlE, the McsA & McsB-induced ClpC ATPase activity was no longer inhibited (Fig 2A).
150 We added this sub-stoichiometric amount of YwlE (0.05 μM) to the *in vitro* disaggregation and
151 refolding assay with ClpC, McsB & McsA (at 1μM) and observed that about 100% of the heat-
152 aggregated Mdh was disaggregated before 90 min, and 50% was successfully refolded after 120
153 min (Fig 2B). Accordingly, pellet-supernatant experiments displayed a clear shift of Mdh from
154 the pellet to the soluble fraction in the presence of ClpC, McsB & McsA with sub-
155 stoichiometric amounts of YwlE (Fig S3A).
156 Interestingly, arginine protein phosphorylation was close to or even below the detection level
157 by western blot analysis, suggesting that sub-stoichiometric amounts of active YwlE are
158 sufficient to lower the phosphorylation state of the involved proteins effectively (Fig S3A).

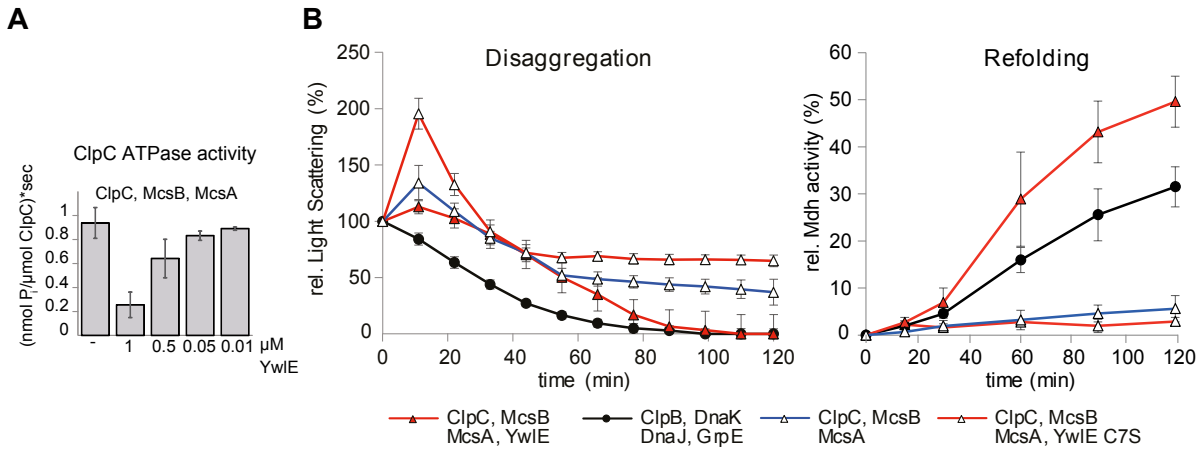

Figure 2 Sub-stoichiometric YwlE facilitates *in vitro* disaggregation and refolding

A) ATPase activity of ClpC/McsB/McsA (1µM) was determined in the absence or presence of indicated amounts of YwlE (0.01-1µM). **B**) Disaggregation and refolding experiments. Disaggregation of heat-aggregated Mdh after the addition of the indicated proteins was monitored *in vitro* by measuring light scattering at 30°C for 120 min (left panel). The refolding was determined by Mdh enzymatic activity (right panel). 0.05 µM YwlE or YwlE C7S were added when indicated. The plots show the mean of at least three replicates with standard deviation.

The addition of the phosphatase inactive YwlE C7S variant (*18*) to the disaggregation and refolding experiment resulted in a low disaggregation rate without apparent refolding (Fig 2B). Consequently, no solubilization of aggregated protein could be observed in the respective supernatant pellet experiment with YwlE C7S (Fig S3A). In the presence of the YwlE C7S variant, the concomitant protein arginine phosphorylation was clearly detectable with a maximum after 15 min, like in the absence of YwlE (Fig 2B & S3A). With order-of-addition experiments, we observed that the later the addition of YwlE was, the lower the disaggregation and the refolding yields were (Fig S4AB).

These experiments suggest that a specific YwlE phosphatase activity is necessary for efficient disaggregation and especially refolding by the ClpC/McsB/McsA chaperone system. YwlE-mediated de-phosphorylation might directly support refolding of unfolded substrate proteins

179 (Fig 2B) and could also modulate ClpC, McsB and McsA activities (*15*, *17*, *20*, *32*) (see Fig
180 6A).

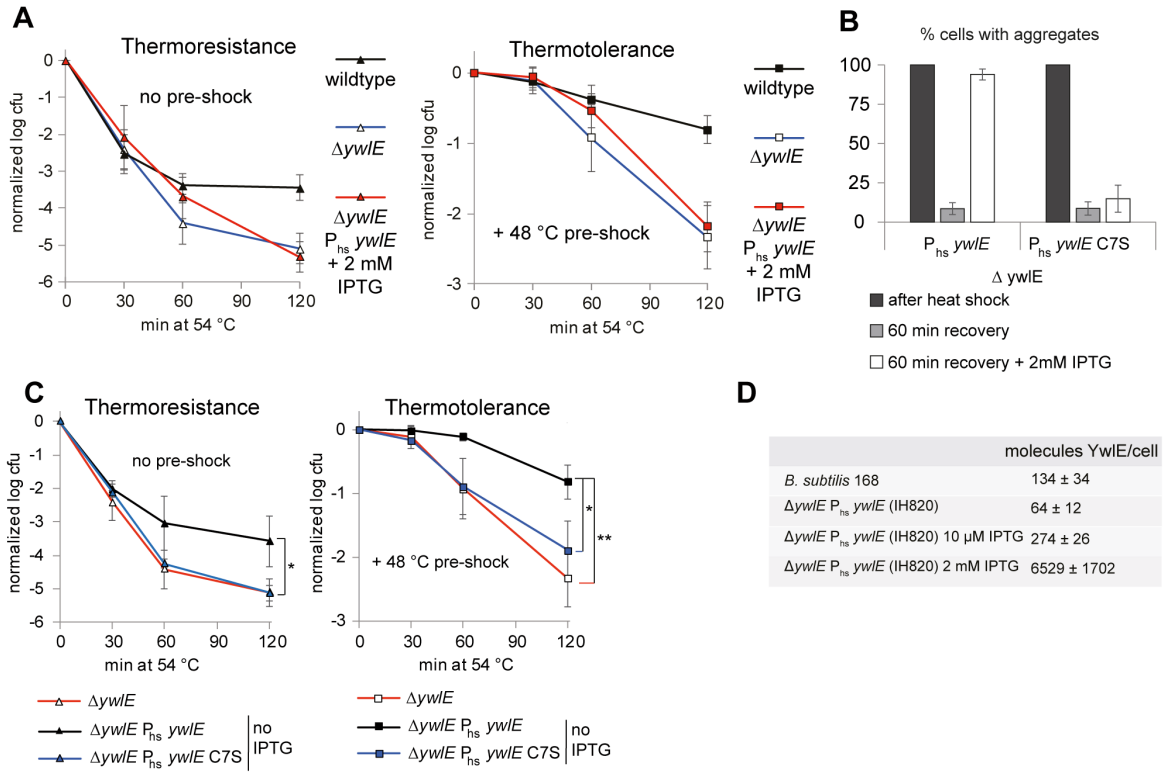

181 **Figure 3 Low *in vivo* levels of YwlE are necessary to facilitate protein homeostasis**
182 **A**) Thermoresistance and thermotolerance experiments with *B. subtilis* wild-type (black), Δ*ywlE* (BIH309,
183 blue) and Δ*ywlE* P_{hs} *ywlE* + 2 mM IPTG (BIH828, red) were performed. Log_{10}-values of viable cell counts
184 were normalized, and three biological replicates were used to calculate standard deviations (error bars). **B**)
185 Subcellular protein aggregates during recovery after heat stress *in vivo*. Cells of *B. subtilis* strains Δ*ywlE* P_{hs}
186 *ywlE* (BIH828) and Δ*ywlE* P_{hs} *ywlE* C7S (BIH829) both also encoding P_{xyl} *yocM-mCherry* were heat shocked
187 for 20 min at 52°C and recovered for 60 min at 37°C. Cells were taken at the indicated time points, and their
188 subcellular protein aggregates analyzed by fluorescence microscopy. Three biological replicates, including
189 three technical replicates with about 50 – 100 cells were analyzed to calculate the ratio of cells containing
190 protein aggregates marked by YocM-mCherry. **C**) Thermoresistance and thermotolerance experiments with
191 *B. subtilis* Δ*ywlE* (BIH309, red), Δ*ywlE* P_{hs} *ywlE* (BIH828, black) and Δ*ywlE* P_{hs} *ywlE* C7S (BIH829, blue)
192 without IPTG. Log_{10}-values of viable cell count were normalized, and three biological replicates were used
193 to calculate standard deviations (error bars) with significant differences indicated (*: $p<0.05$, **: $p<0.01$,
194 ***: $p<0.001$, Welch's test). **D**) Table showing the number of YwlE proteins/cell determined *in vivo* by
195 quantitative Western blotting for the different *B. subtilis* strains at indicated IPTG concentrations (see Fig
196 S3E).
197

198 **A well-balanced YwlE level is necessary for functioning *in vivo* protein homeostasis**

199 The sub-stoichiometric levels of YwlE relative to the ClpC chaperone complex from the *in vitro*
200 experiment of about 1:20-1:30 (Fig 2) correspond relatively well to the observed *in vivo* ratio
201 of about 20 to 100 times lower cellular concentration of YwlE, compared to the higher abundant

202 ClpC determined *in vivo* for *B. subtilis* cells by different methods in various conditions (*14*, *33*,
203 *34*).
204 Since the relative levels of the YwlE phosphatase appear to be important for the *in vitro*
205 disaggregation and refolding, we went on to investigate the effect of different cellular *in vivo*
206 levels of YwlE on protein homeostasis and heat shock response. For this, we used the Δ*ywlE*
207 mutant strains where we could control cellular YwlE levels with an IPTG inducible expression
208 of *ywlE* or *ywlE* C7S *in trans*. We measured the cellular YwlE levels of wild-type *B. subtilis*
209 and these strains by quantitative western blotting and observed about 134 (±34) YwlE
210 molecules per cell in wild-type and 64 (±11) in the complemented Δ*ywlE* P_{hs} *ywlE B. subtilis*
211 strain without induction (Fig 3D & Fig S3E). The addition of 10 µM IPTG doubled the cellular
212 YwlE to 274 (± 26) molecules/cell and reached about 6500 (± 1702) YwlE molecules per cell
213 when 2 mM IPTG was added (Fig 3D & S3E). Interestingly, the uninduced Δ*ywlE* P_{hs} *ywlE*
214 strain with almost wild-type levels of YwlE behaved like the wild-type in thermotolerance and
215 thermoresistance experiments. The more IPTG inducer was added, the more YwlE was
216 expressed and the less thermoresistant or thermotolerant these cells became (Fig 3AC & S3C).
217 However, thermotolerance and thermoresistance were as low as in a Δ*ywlE* strain when
218 complemented with the phosphatase inactive *ywlE* C7S variant (Fig 3C). Assessing the
219 subcellular aggregate formation revealed increased subcellular aggregates at 48°C and 48/53°C
220 during thermotolerance for the cells with increased *ywlE* expression but not when *ywlE* C7S
221 was expressed (Fig S3B). Furthermore, high levels of *ywlE* diminished the clearance of heat-
222 induced aggregates during recovery from heat stress (Fig 2D), which was not observed with
223 low YwlE levels or for the Δ*ywlE* strain complemented with the highly expressed *ywlE* C7S
224 (Fig 3B).
225 We did not observe an influence of *ywlE* expression on the level of subcellular aggregates
226 during recovery from heat stress in a kinase-inactive *mcsB*C167S mutant (Fig S3D), confirming

227 that the presence of protein arginine phosphorylation activity is required to observe an influence
228 of the counteracting *ywlE* phosphatase activity.
229 High levels of YwlE phosphatase interfered strongly with the McsB kinase and thereby
230 appeared to behave like a strain lacking McsB (Fig S2AB & Fig3AC) both *in vitro* and *in vivo*.
231 Controlling the cellular levels of protein arginine phosphorylation is therefore not only
232 mediated by the McsA-activated McsB kinase but also controlled by the YwlE phosphatase,
233 facilitating a well-balanced equilibrium of cellular protein arginine phosphorylation levels to
234 maintain cellular protein homeostasis.

235 **The YwlE-dependent *in vitro* refolding is independent of the ClpC unfolding activity**

236 To assess the interplay of the ClpC chaperone activity and the refolding facilitated by the YwlE
237 phosphatase, we used a ClpC trap variant (ClpC-DWB), which cannot hydrolyze ATP. ClpC-
238 DWB can form mixed oligomers with ClpC and can thereby interfere with the ATPase driven
239 activities of ClpC (Fig S4C & S4D) (*35–38*). The addition of ClpC-DWB to our *in vitro* assay
240 with ClpC, McsA & McsB 15 min after the start, resulted in a slow decline to a lower but
241 constant light scattering signal for the remaining time (Fig S4C), suggesting that the
242 disaggregation was halted (*36*). The simultaneous or subsequent addition of YwlE (at 15 (green
243 squares) or 20 min (blue diamonds)) appeared to disrupt the apparent complex much faster,
244 resulting in a drop to the same lower level of constant light scattering (Fig S4C). Importantly,
245 the addition of active YwlE could facilitate up to 15 % recovery of enzyme activity after 120
246 min (green squares). However, no considerable refolding occurred when YwlE C7S variant was
247 added (purple circles) (Fig S4C). These experiments suggest that the YwlE phosphatase activity
248 is necessary to support the refolding of the available unfolded and phosphorylated substrate
249 proteins independent of a concurrent ClpC ATPase-driven unfoldase activity (Fig S4C).

250 **McsA is necessary for starting the disaggregation and refolding activity**

251 We could demonstrate that adding McsA at different time points to McsB, ClpC and YwlE
252 immediately increased the light scattering signal suggesting an initial protein complex

253 formation, followed by the onset of the disaggregation reaction and Mdh activity starting to
254 become recovered (Fig S4E). At the same time, the start of protein arginine phosphorylation of
255 the involved proteins could be detected, confirming the concurrent activation of the McsB
256 kinase activity by McsA (Fig S4F) (*19*). These experiments suggest that the McsA interaction
257 with McsB and its kinase activation is necessary to initiate the efficient disaggregation and
258 subsequent refolding activity by this chaperone system.

259 **ClpP association with ClpC: allowing a switch between repair or removal?**

260 ClpC and ClpP can form the ClpCP AAA+ protease complex (*39–42*). Therefore, we
261 investigated how the presence of ClpP influences the disaggregation and refolding activity of
262 McsB, McsA, ClpC, and YwlE (Fig 4A) and to what extent this repair activity would shift
263 toward substrate degradation (Fig 4B).

264 Adding ClpP in the absence of YwlE significantly enhanced the disaggregation activity (Fig
265 4A, green squares), and about 90% of aggregated Mdh was degraded (Fig 4B). Still, about 10%
266 of the aggregated Mdh was refolded (Fig 4A, green squares). The raised disaggregation activity
267 (Fig 4A) is consistent with the observed concurrent induction of the ClpC ATPase activity when
268 ClpP was added (Fig S5A). The additional presence of YwlE did not further influence
269 disaggregation efficiency but resulted in about 40 % refolding of the aggregated Mdh (Fig 4A,
270 blue circles), similar to the reaction in the presence of YwlE but without ClpP (Fig 4A, red
271 triangles). At the same time, about 60% of the initial aggregated Mdh (Fig 4A, blue circles)
272 was degraded (Fig 4B). These *in vitro* experiments suggest a triage where the refolded Mdh
273 species could escape the transfer to the associated ClpP protease, but the still unfolded substrate
274 proteins were successfully transferred for degradation into the ClpP protease complex.

275 The ClpC association with ClpP is mediated by the tips of ClpP-interacting loops (P-loops)
276 extending from the bottom of the AAA+ protein hexamer and interacting with binding pockets
277 on the apical surface of the double-heptameric ClpP complex (*6*, *39*, *40*, *42*, *43*). The P-loop of

ClpC contains a VGF motif at its tip, while other Clp proteins like ClpX from *B. subtilis* and *E. coli* possess IGF P-loops to facilitate this interaction.

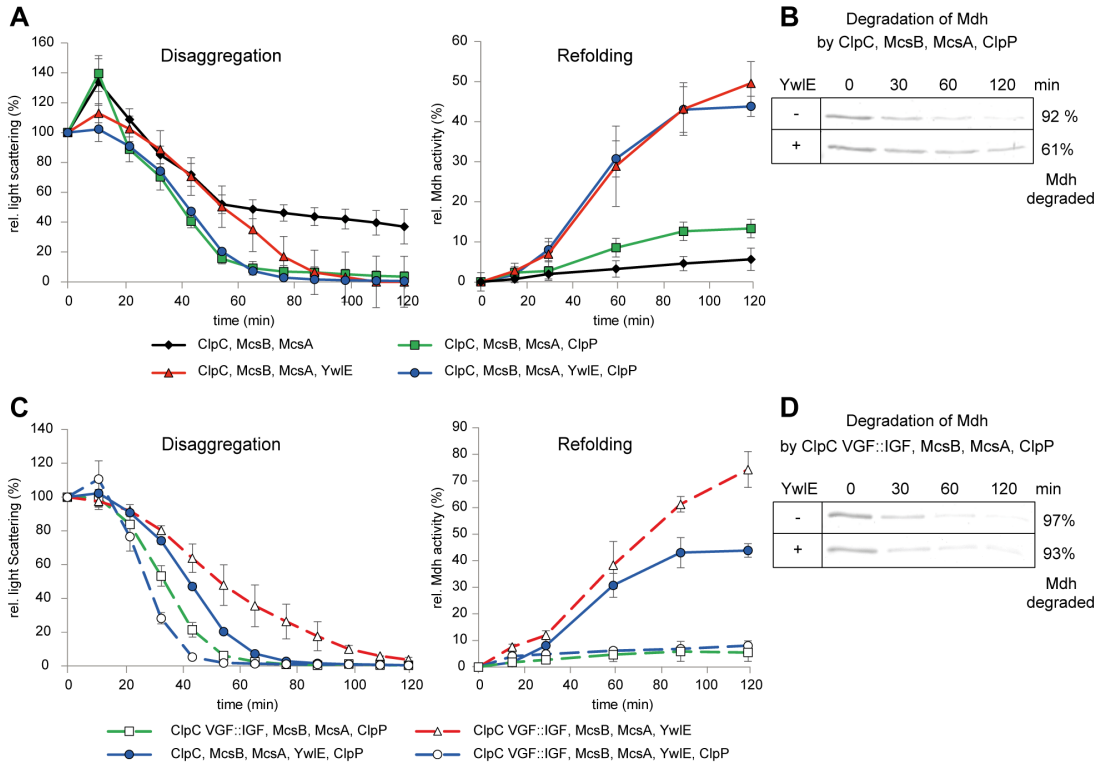

Figure 4 ClpCP interaction strength and the influence of YwlE on refolding or degradation

Disaggregation, refolding and degradation experiments. **A**) After the addition of the indicated proteins, disaggregation of heat-aggregated Mdh (1 µM) was monitored *in vitro* by measuring light scattering (left panel) and refolding by measuring the Mdh enzymatic activity (right panel). **B**) *In vitro* degradation experiments of heat aggregated Mdh as substrate were performed with the indicated proteins. Samples were taken for analysis by SDS PAGE and Coomassie stain. The relative amount of degraded Mdh after 120 min is indicated. **C**) Disaggregation of heat aggregated Mdh (1 µM) was monitored *in vitro* after the addition of the indicated proteins by measuring light scattering (left panel) and refolding by measuring the Mdh enzymatic activity (right panel) **D**) *In vitro* degradation experiments of heat-aggregated Mdh as substrate were performed with the indicated proteins. Samples were taken for analysis by SDS PAGE and Coomassie stain. The relative amount of degraded Mdh after 120 min is indicated.

Interestingly, it was demonstrated that in the context of *E. coli* ClpXP, the ClpX IGF loop allows a tighter interaction between ClpX and ClpP than a VGF loop (*39*). To further evaluate the difference between the VGF vs IGF P-loop for the interaction of ClpC with ClpP, we utilized the recently resolved structure of a ClpX-ClpP complex from *Listeria monocytogenes* (*44*) and the *B. subtilis* ClpP structure (*45*), to model and calculate thermodynamic interaction parameters of the IGF compared to the VGF P-loop for ClpP binding. These *in silico* modeling

300 and calculations suggested a stronger binding interaction of the IGF P-loop than the VGF P-
301 loop (Fig S5E). When we replaced the Valine in the VGF motif with Isoleucine, we observed
302 in our *in vitro* experiments that the ClpC VGF::IGF variant in the presence of McsB and McsA
303 displayed a slightly lower ATPase (Fig S5B) and a lower disaggregation activity (Fig 4C), and
304 a high refolding activity of up to 80% in the presence of YwlE (Fig 4C). Adding ClpP to
305 ClpC VGF::IGF with McsB and McsA enhanced the disaggregation activity and switched the
306 proteolytic activity of this complex to a full degradation of Mdh, independent of the presence
307 of YwlE (Fig 4D, Fig S5D). The observed complete degradation of the substrate protein by the
308 ClpC VGF::IGF/ClpP AAA+ protease complex (Fig 4D) contrasts the only partial degradation
309 of the remaining unfolded substrate protein with wild-type ClpC (Fig 4B). This difference
310 suggests that a closer and possibly tighter interaction of ClpC VGF::IGF with ClpP might
311 interfere with the escape of already folded substrate protein observed for wild-type ClpC-ClpP
312 (Fig 4AB).
313 Such a relatively transient, more dynamic ClpC-ClpP interaction during disaggregation and
314 unfolding would give better access to the YwlE phosphatase for the de-phosphorylation of
315 translocated phosphorylated unfolded protein substrates. And it could allow at the same time, a
316 more unconstrained folding of the extruding nascent polypeptide chains (see Fig 6B).

317 **The ClpCP AAA+ protease complex formation is not necessary for protein homeostasis**
318 **during heat shock but beneficial during more severe proteotoxic stress.**

319 Our *in vitro* experiments suggest that the ClpCP complex can switch between a refolding and
320 a degradation mode, depending on the interaction strength of its P-loop with ClpP (Fig 4). To
321 investigate the role of ClpC/ClpP interaction *in vivo*, we constructed a *B. subtilis* mutant strain,
322 encoding a P-loop ClpC VGF::GGR variant, which abolishes the interaction with the ClpP
323 complex and has, therefore, no proteolytic activity towards known substrates neither *in vivo* nor
324 *in vitro* (Fig S6AB) (*14*, *15*). However, it is active in the *in vitro* disaggregation and refolding
325 experiment (Fig S6E), with a slightly lower ATPase compared to ClpC (Fig S6D).

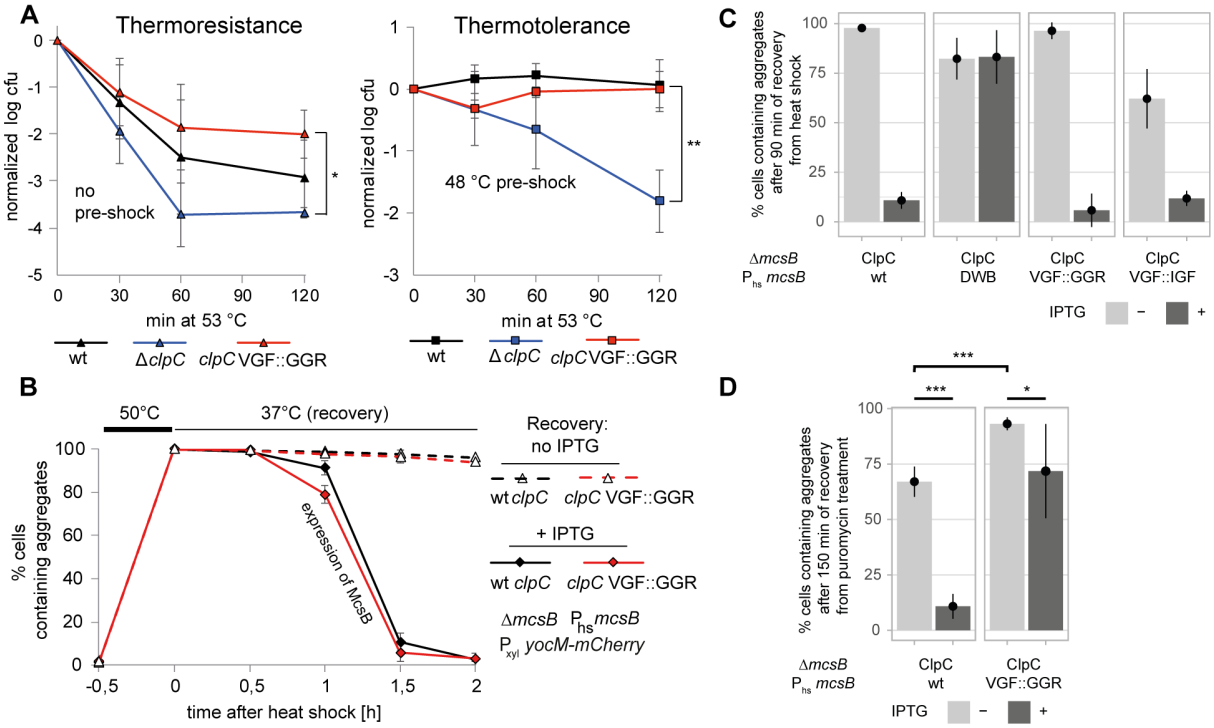

Figure 5 ClpC P-loop variants: rescue or removal?

A) Thermoresistance and thermotolerance experiments with *B. subtilis* wild-type (black), Δ*clpC* (BIH19, blue) and *clpC* VGF::GGR (BIH217, red) cells. Log_{10}-values of viable cell count were normalized, and three biological replicates were used to calculate standard deviations (error bars). Significant differences are indicated (*: p<0.05, **: p<0.01, ***: p<0.001, Welch's test). **B**) Cells of *B. subtilis* ClpC wt (BIH414, black) and ClpC VGF::GGR (BIH485, red) (with Δ*mcsB* P_{hs} *mcsB* P_{xyl} *yocM-mCherry*), were treated with a 50°C heat shock and subsequently shifted to recover at 37°C. The ratio of cells containing protein aggregates were determined. **C**) ClpC wt (BIH414), ClpC-DWB (BIH488), ClpC VGF::GGR BIH485) and ClpC VGF::IGF (BIH860) strains (and Δ*mcsB* P_{hs} *mcsB* P_{xyl} *yocM-mCherry*) were treated with a 50°C heat shock and shifted for 90 min to 37°C in the absence or presence of IPTG. The ratio of cells containing protein aggregates was determined. Three biological replicates, including three technical replicates with 50 – 100 cells, were analyzed. Log_{10}-values of viable cell count were normalized, and three biological replicates were used to calculate standard deviations (error bars). **D**) *B. subtilis* ClpC wt (BIH414) and ClpC VGF::GGR (BIH485) were treated with 25 µg/mL puromycin. After 15 min, puromycin was removed, and the cells were incubated in fresh media with xylose in the presence or absence of 2 mM IPTG at 37 °C for 150 min. Samples were taken for analysis by fluorescence microscopy and western blot analysis (see also S6F & G). The ratio of cells containing protein aggregates was determined based on three biological replicates, including three technical replicates with 50 – 100 cells. Log_{10}-values of viable cell count were normalized and three biological replicates were used to calculate standard deviations (shown as error bars) with significant differences indicated (*: p<0.05, **: p<0.01, ***: p<0.001, Welch's test).

While a Δ*clpC* deletion mutant showed impaired thermotolerance development, less thermoresistance and increased protein aggregation during heat shock (*9–11*), a *clpC* VGF::GGR and the *clpC* VGF::IGF mutant strain behaved comparable to the wild-type strain in thermoresistance, thermotolerance (Fig 5A & Fig S5C) and protein aggregate formation (Fig S6C). In addition, McsB-mediated removal of heat-induced protein aggregates during recovery

353 from heat shock was not affected in a wild-type or a *clpC* VGF::GGR, but strongly impaired in
354 the *clpC* DWB background strain (Fig 5BC). Interestingly, fewer subcellular protein aggregates
355 were detected in the *clpC* VGF::IGF mutant strain already without induction of McsB
356 expression. However, upon full McsB induction, they were removed to the same level as in the
357 wild-type ClpC control (Fig 5C).
358 We also applied a more severe protein folding stress by adding the antibiotic puromycin, a
359 tRNA mimic whose presence results in premature translation termination, generating easily
360 aggregating non-functional protein fragments (Fig 5D & Fig S6F). After removing puromycin,
361 we observed the clearance of protein aggregates in the *mcsB* deletion mutant after 150 min,
362 only when *mcsB* expression was induced (Fig 5D & Fig S6F). However, the clearance of these
363 truncated protein aggregates was strongly diminished in the *clpC* VGF::GGR mutant (Fig 5D
364 & Fig S6F).
365 These experiments demonstrated that the ClpC VGF::GGR variant, although not able to
366 associate with ClpP, could very well replace wt ClpC as unfoldase, also during heat shock
367 response, however, not when more toxic not refoldable protein aggregates were present (Fig
368 5ABC, Fig S6C). This suggests that switching to ClpCP-mediated degradation can be beneficial
369 under more severe protein folding stress (Fig 6).

370 **Discussion**

371 Here, we could identify and describe an unusual AAA+ chaperone system, which integrates
372 protein modification and de-modification to enhance and facilitate cellular protein homeostasis.
373 In this chaperone system, the cellular level of protein arginine phosphorylation is controlled by
374 sub-stoichiometric level of the YwlE phosphatase. Thereby the McsB kinase activity and
375 cellular protein arginine phosphorylation can be limited, which allows the modulation of ClpC-
376 mediated disaggregation and unfolding activities and the additional subsequent facilitation of
377 substrate refolding (Fig 2 & 3). The specific targeting of misfolded or aggregated protein by
378 McsB (*28*) (Fig 1, 2, & S2) is consistent with the previous identification of a wide array of

379 cellular proteins, which can become modified by protein arginine phosphorylation, since they
380 might be prone to aggregation (*17*, *20*).
381 The kinase activity of the McsB adaptor protein adds complexity but also expands the
382 recognition and targeting abilities of McsB. The activation of ClpC by McsB can be facilitated
383 by binding to the NTD of ClpC, but ClpC can be further activated by phosphorylation of
384 specific arginine residues located in the NTD of ClpC (*17*, *20*, *22*). We could observe a basal
385 adaptor protein activity for the kinase-inactive McsB C167S variant (Fig S2). Both McsB and
386 McsB C167S interact with the NTD of ClpC, and both recognize sub-cellular protein aggregates
387 (Fig S2) and can directly target misfolded or aggregated substrate proteins to ClpC, even when
388 the substrate proteins lack arginines (*15*, *17*, *24*). This ability of McsB would also allow the
389 recruitment of ClpC to these substrate protein structures (*15*, *28*), similar to DnaK, which can
390 act as an adaptor protein for the ClpB disaggregase (*46*).
391 A distinct substrate recognition and targeting pathway involving the McsB kinase was reported,
392 where McsB is not necessarily interacting directly with ClpC. Here the phospho-arginine
393 modifications of unfolded substrate proteins, generated directly by the McsB kinase, can act as
394 a degron, which allows the direct recognition of the marked substrate proteins via specific
395 phospho-arginine interaction sites in the NTD of ClpC (*21*, *22*, *25*). This additional second
396 recognition path for soluble substrate could play a role for a more efficient function of the
397 chaperone complex since unfolded phosphorylated substrate proteins that exit ClpC and are
398 neither dephosphorylated by YwlE, nor degraded by ClpP could then become directly
399 retargeted by their still present degron to ClpC unfolding (*22*) (Fig 6).
400 The arginine phosphorylation of unfolded, misfolded, or aggregated protein species might
401 change the physical properties of these protein species in different ways. Arginine
402 phosphorylation reverts a positive to a negative charge, which can result in obliterating
403 unspecific or specific interaction with DNA or RNA (*16*). Protein aggregates with these
404 differently charged misfolded phosphorylated protein species might be physically better

405 accessible. And ClpC could also interact directly via its phospho-arginine receptors of the NTD
406 with protein arginine phosphorylated misfolded proteins exposed on the surface or in the
407 vicinity of such protein aggregates (*22*).
408 We observed that the YwlE phosphatase was essential to facilitate the refolding of the unfolded
409 phosphorylated protein substrates extruded from the ClpC chaperone system (Fig 2 & 4). Here
410 we hypothesize that the released unfolded and phosphorylated substrate protein species might
411 be unable to refold successfully. However, in the presence of YwlE, the phosphoryl group can
412 be removed, possibly allowing the refolding of the substrate protein, which is somehow
413 reminiscent of the classical refolding experiments by Anfinsen (*47*).
414 Notably, a high-energy P-N bond is formed in phospho-arginine by McsB (*16*, *48*). This might
415 be an important aspect when considering possible thermodynamic requirements of the folding
416 process accompanying the YwlE-mediated protein arginine de-phosphorylation.
417 Different combinations of specific Hsp40, Hsp70, and Hsp110 chaperone systems or AAA+
418 unfoldases, such as ClpB (Hsp104) combined with Hsp70, were demonstrated to remove
419 protein aggregates by disaggregation and refolding in their respective cellular systems. Some
420 AAA+ unfoldases, such as ClpG, even displayed a stand-alone disaggregation and refolding
421 activity (*5*, *49*, *50*).
422 Here the ClpC AAA+ chaperone system supported by adaptor proteins such as MecA (Fig S1)
423 or the kinase-inactive McsB C167S with McsA (Fig S2), could, to a certain extent, facilitate a
424 disaggregation and refolding activity. However, coupling the ClpC-mediated unfolding to
425 protein arginine phosphorylation and de-phosphorylation by McsB, McsA & YwlE resulted in
426 an improved disaggregation and a significantly increased refolding activity (Fig 2). This
427 suggests a synergy between the ClpC-mediated generation of unfolded extruding polypeptide
428 chains, its concurrent McsB-mediated modification and the subsequent YwlE-catalyzed de-
429 modification.

430 Protein stability, folding and function are known to be intricately connected to post-translational
431 protein modification (*51*, *52*). It is well established that protein modification by glycosylation
432 and de-glycosylation play an important role in protein homeostasis in the endoplasmic
433 reticulum (*53–55*). Interestingly, ubiquitination and de-ubiquitination by the deubiquitinating
434 enzyme USP19 were suggested to support membrane protein folding at the cytosolic side of the
435 ER membrane (*56*).

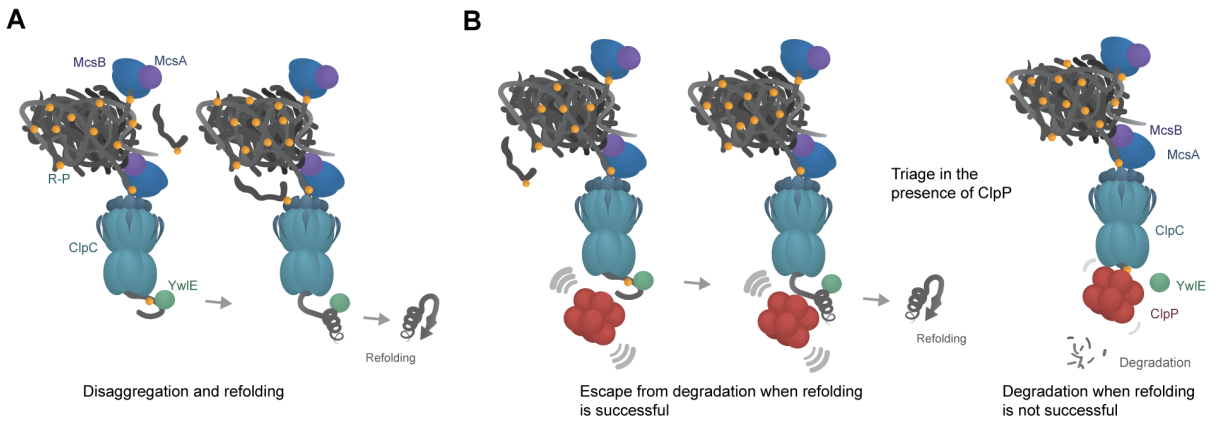

436

437 **Fig 6 Disaggregation and refolding or degradation**
438 **A)** Model for the disaggregation and refolding in the absence of ClpP. **B)** Model for the triage in the presence
439 of ClpP: Escape from transfer to degradation by extruded and simultaneously refolded protein substrates
440 (left). Degradation of not folded protein substrates.
441
442 In the presence of ClpC-associated ClpP, unfolded or misfolded substrate proteins are targeted
443 for ClpP degradation. However, already folded protein species are not transferred for
444 degradation, due to the dynamic interaction of the P-loops with the ClpP oligomer (Fig 4). Such
445 a relatively loose ClpC-ClpP interaction could allow YwlE access to the egressing unfolded
446 peptide from ClpC to facilitate refolding by removing the possibly interfering arginine
447 modification. This suggests that the McsB/McsA/ClpCP/YwlE complex can switch between
448 repair or degradation, depending on the folding kinetics or state of the modified or already
449 demodified nascent polypeptide chain unfolded and translocated by ClpC (Fig 6).
450 In the presence of the YwlE phosphatase, ClpC, McsB, and McsA establish a unique and
451 effective disaggregation and refolding system, employing reversible protein arginine
452 modification for various tasks, including substrate protein refolding. This ability to remove or

453 repair stress-induced cellular protein aggregates allows to maintain protein homeostasis and is
454 giving the bacterial cells the means to respond and withstand protein misfolding stress.

455 **Materials & Methods**

456 **General methods**

457 *B. subtilis* strains were grown in Lysogeny Broth medium (5 g l^{-1} yeast extract, 10 g l^{-1}
458 tryptone-peptone, 5 g l^{-1} NaCl) at 37°C. Supplemental Table S1 shows the strains derived from
459 transformations of indicated plasmids or PCR products (Table S2) derived from cloning with
460 primers/restriction enzymes (Table S3) with standard cloning procedures (restriction enzymes
461 and T4 DNA ligase from NEB) as described previously (*57*). Cloning was performed in *E. coli*
462 DH5α (Invitrogen) (ampicillin 100 µg ml^{-1}, kanamycin 50 µg ml^{-1}) with Phusion High Fidelity
463 Polymerase (NEB). Transformation into *B. subtilis* with chromosomal or plasmid DNA was
464 performed by standard methods (*58*). Successful *amyE* insertion in *B. subtilis* was identified by
465 assessing α-amylase activity on plates with 0.4 % starch (w/v) and Lugol's iodine. Insertions in
466 *amyE* and other genomic sites such as *lacA* were confirmed by PCR.

467 **Protein purification**

468 Protein production was performed in *E. coli* BL21 (DE3) cells. Cells were grown at 37°C to an
469 OD_{600} of 0.7 and induced with 1 mM IPTG overnight at 16°C. Purification of His_6-tagged
470 proteins was performed by nickel affinity chromatography after cell lysis by French press.
471 YocM, McsB and McsB C167S were expressed and purified as N-terminal His-SUMO fusion
472 proteins, which were released by overnight cleavage with Ulp-protease at 4°C (Andréasson et
473 al., 2008). ClpC, ClpC-DWB, ClpC-VGF:IGF, ClpC-VGF:GGR, ClpP, MecA, McsA, YwlE
474 and YwlEC7S were purified as previously described (*19*, *36*).

475 **Thermotolerance development and thermoresistance**

476 Thermotolerance development and thermoresistance experiments were performed as previously
477 described (*9*, *59*). Cell cultures were separated at OD_{600} 0.4 and treated ± a 15 min pre-shock

478 of 48°C before both samples were shifted to 53°C or 54°C. Samples were taken for microscopy
479 or plated on LB agar at t_0, t_{30}, t_{60} and $t_{120\ min}$. Obtained *cfu* were plotted against time. At least
480 three biological replicates were used to calculate standard deviations, and statistical
481 significance was calculated using Welch's test.

482 **Fluorescence microscopy**

483 *B. subtilis* cells were inoculated with a fresh overnight culture to an OD_{600} of 0.05 in LB +
484 0.5 % xylose (w/v) to express *yocM-mCherry* fusion (*9*). Fluorescence microscopy was
485 performed at indicated time points on an object slide coated with 1 % agarose (w/v) in saline
486 (0.9 % NaCl (w/v)). Oil immersion and 10x100 magnifications were used with a Zeiss
487 fluorescence microscope with GFP and mCherry filters.

488 ***In vivo* disaggregation assay**

489 *B. subtilis* strains grown in LB + 0.5 % xylose (w/v) were treated at OD_{600} 0.25 – 0.3 with a
490 heat shock at 52°C for 20 min or 50°C for 30 mins if the strain lacks *mcsB*, which renders them
491 more sensitive towards heat stress (Fig 1C). Cultures were separated and ± 2 mM IPTG was
492 added while shifting the cells to 37°C. Samples were taken for plating (colony forming units
493 (CFU)), western blotting and/or fluorescence microscopy as indicated. At least three biological
494 replicates were used to calculate standard deviations, and statistical significance was calculated
495 using Welch's test.

496 **Biochemical assays**

497 Light scattering and Mdh activity assays: Malate dehydrogenase (Roche) was inactivated and
498 aggregated by incubating 2 µM for 30 min at 47°C. Light scattering was determined at 360 nm
499 excitation and emission wavelength with a FP-6500-Spectrofluorometer (Jasco) at 30 °C.
500 1.5 µM ClpB, 1 µM DnaK, 0.2 µM DnaJ, 0.1 µM GrpE, 1.5 µM ClpC, 1 µM ClpP, 1 µM
501 MecA, 1 µM McsB, 1 µM McsA, 0.05 µM YwlE, proteins were incubated as indicated in the
502 respective experiments with 1 µM heat-treated Mdh in refolding buffer (50 mM Tris pH 7.8,

503 150 mM KCl, 20 mM $MgCl_2$, 2 mM DTT) supplemented with 20 µg/ml pyruvate kinase, 4 mM
504 phosphoenolpyruvate and 6 mM ATP as indicated in the respective experiments.
505 Mdh enzyme activity was determined before and after inactivation and at indicated time points
506 by diluting 2.5 µl reaction mixture in 125 µl Mdh activity buffer (150 mM potassium phosphate
507 buffer pH 7.6, 1 mM DTT, 0.5 mM oxalacetate, 0.28 mM NADH). The time-dependent NADH
508 oxidation by Mdh was monitored at 340 nm in a Spectra Max MP3 Microplatereader
509 (Molecular Devices). At least three replicates of these experiments were analyzed, and the
510 resulting standard deviation was included as error bars.
511 We also followed the solubilization of aggregated proteins by supernatant pellet experiments.
512 Samples of the disaggregation and refolding experiments were taken at indicated time points,
513 and centrifuged for 30 min, 14000 rpm at 4°C. The supernatant was carefully separated from
514 the pellet and mixed with the appropriate amount of 2x SDS sample buffer while the pellet was
515 dissolved in 1x SDS sample buffer to the same final volume. Both samples were incubated for
516 10 min at 90°C and analyzed via SDS-PAGE and Coomassie stain (Schlothauer et al., 2003).
517 The in vitro degradation of aggregated Mdh or β-casein in the presence of ClpP was analyzed
518 by SDS-PAGE and Coomassie stain. The relative amount of Coomassie-stained protein band
519 was calculated using ImageJ analysis software to determine band intensities (*60*).
520 The ClpC ATPase activity was measured by phosphate release, colorimetrically detected with
521 the ammonium molybdate/malachite green assay as described previously (*61*, *62*). For this
522 assay we used 1 µM ClpC, 1 µM ClpP, 1 µM MecA, 1 µM McsB, 1 µM McsA, 0.05 µM YwlE,
523 and possible substrates such as 1 µM Mdh, 1 µM β-casein, as indicated and if not mentioned
524 otherwise. At least three replicates of the ATPase experiments were implemented, and the
525 resulting standard deviation was included as error bars.
526 **Western blotting**
527 SDS PAGE (15 % gels) loaded with similar amounts of protein (e.g. 5 µg total protein for cell
528 extracts) was performed with standard methods as previously described (Laemmli 1970) with

529 anti-YwlE, anti-ClpC, anti-MecA, anti-McsB or anti-YpbH (Pineda Berlin) antiserum as
530 primary antibody and anti-rabbit alkaline phosphatase or horseradish peroxidase conjugate as
531 secondary antibody (1:10000). Blots were developed with standard BCIP (5 % (w/v) in DMF)
532 + 250 µL NBT (5 % (w/v) in 70 % DMF) or using the ECL western blotting reagent (GE
533 Healthcare).
534 For phospho-arginine protein detection, samples were taken from light scattering assays
535 without heat treatment prior to loading. SDS-PAGE and western blotting on nitrocellulose were
536 performed at 4 °C. The primary anti-phosphoarginine-specific antibody was used 1:3000 with
537 5 % skim milk powder in TBS. Secondary antibodies and imaging was performed as described
538 above (*31*). hs
539 **YwlE quantification**
540 *B. subtilis* 168 (wild-type) and IH820 (Δ*ywlE*::*kanR* P_{hs} *ywlE* spec) cells were grown to an OD
541 0.35 ± 0.02. Subsequently, IPTG was added to a final concentration of 0.01 and 2 mM IPTG to
542 the IH820 cultures as indicated, which were further incubated for 30 min (Fig S3C). To
543 determine the number of bacteria, an aliquot was fixed with 3.7% formaldehyde in PBS and
544 cells were counted in a Petroff-Hauser chamber. Cell extracts were prepared by sonication and
545 western blotting was performed as mentioned above with few modifications. Samples were
546 resolved in 4-15% Mini-PROTEAN TGX precast gels and transferred to 0.22 µm PVDF
547 membranes. Anti-YwlE serum was used in a 1:5,000 dilution in 5% skim milk in TBS-T, and
548 anti-rabbit IgG antibodies from goat conjugated to HRP were used 1:20,000 in the same buffer.
549 Blots were developed using a chemiluminescent substrate (Thermo Scientific, 34577) and
550 documented in a Fusion FX imaging system (Vilber). Defined amounts of purified YwlE-His
551 were included as a calibration curve on each gel (Fig S3C). The concentration of purified YwlE-
552 His was quantified by MS. Briefly, defined amounts of synthesized heavy isotope-coded YwlE
553 peptides (Table S4; JPT Peptide Technologies, Berlin) were spiked into a sample of the purified
554 YwlE protein. The concentration of the YwlE protein was then determined by dividing the MS

555 signal of the endogenous "light" peptides by the synthetic "heavy" peptides. Western blot
556 images were processed using Fiji (*63*).

557 **Structure modelling**

558 As a structural template for modelling the ClpC-ClpP interactions, we used the ClpP-ClpX
559 complex structure (PDB IDs: 6SFW, 6SFX) (*44*). Each ClpX subunit and the two interacting
560 ClpP subunits were extracted, and energy minimization was performed using RosettaScripts
561 (*64*) with the FastRelax (*65*) mover and strong coordinate constraints. To compare binding
562 energies, the wild-type and ClpX I265V (or IGF::VGF) mutant were again minimized, only
563 allowing the backbone of the IGF-loop to move in an unconstrained manner. Binding energies
564 (ΔΔGbind) were calculated with the Rosetta energy function as ΔG complex – (ΔG ClpP,
565 separated + ΔG ClpC/X,s eparated) using the Rosetta Interface Analyzer application, allowing
566 side chains to re-pack in the separated interactions partners. To estimate the difference in
567 binding in the *B. subtilis* ClpC-VGF and ClpC-IGF, the *B. subtilis* ClpP structure representing
568 the open conformation (PDB ID: 3KTK) (*45*) was structurally aligned to 6SFX to have the *L.*
569 *monocytogenes* ClpX IGF loops placed onto ClpP analogous to the *L. monocytogenes* ClpP-
570 ClpX complex structure. Due to the symmetry mismatch between ClpP and ClpX, the six IGF
571 loops were bound in distinct conformations, five of which are relatively similar (conformation
572 1), whereas one loop has a different conformation (conformation 2) (Fig S5E). In all
573 conformations, changing Ile to Val diminishes the calculated binding energy (Fig S5E). Energy
574 minimization and binding energy calculations were done as described above.

575

576 **Author contributions** RA, IH, NM, EC & KT were involved in conceptualization. RA, IH,
577 FAC, KG & NM designed and performed the experiments. SR performed the *in silico* analysis
578 for the binding energies. IH, RA, FAC & KT wrote the initial manuscript. All authors
579 contributed to the manuscript writing, experimental design and analyzed the data. EC & KT
580 supervised the study and were responsible for funding acquisition.

581 **Funding** Work in our Lab was supported by the Deutsche Forschungsgemeinschaft (Tu106/6,
582 Tu106/8 (SPP1879) to KT & Leibniz-Price to EC) the Max Planck Society (EC & KT) and a
583 PhD fellowship from the Hannover School for Biomolecular Drug Research (HSBDR) to IH.
584 **Acknowledgements** We want to thank Jakob Fuhrmann (Scripps Research Institute) & Paul
585 Thompson (University of Massachusetts Medical School) for samples of the anti-phospho-
586 arginine antibody. David Dubnau (PHRI, Newark, NJ) & Axel Mogk (ZMBH, Uni Heidelberg)
587 for strains and plasmids. Alex Elsholz (MPUSP, Berlin) for discussion. Christian Frese and
588 Florian Kondrot (MPUSP, Berlin) for proteomic analysis.

589 **References**

590 1. A. Battesti, S. Gottesman, Roles of adaptor proteins in regulation of bacterial proteolysis. *Curr.*
591 *Opin. Microbiol.* **16**, 140–147 (2013).

592 2. F. U. Hartl, A. Bracher, M. Hayer-Hartl, Molecular chaperones in protein folding and proteostasis.
593 *Nature*. **475**, 324–332 (2011).

594 3. J. Kirstein, N. Molière, D. A. Dougan, K. Turgay, Adapting the machine: adaptor proteins for
595 Hsp100/Clp and AAA+ proteases. *Nat. Rev. Microbiol.* **7**, 589–599 (2009).

596 4. A. Mogk, D. Huber, B. Bukau, Integrating protein homeostasis strategies in prokaryotes. *Cold*
597 *Spring Harb. Perspect. Biol.* **3** (2011), doi:10.1101/cshperspect.a004366.

598 5. A. Mogk, B. Bukau, H. H. Kampinga, Cellular Handling of Protein Aggregates by Disaggregation
599 Machines. *Mol. Cell*. **69**, 214–226 (2018).

600 6. R. T. Sauer, T. A. Baker, AAA+ proteases: ATP-fueled machines of protein destruction. *Annu. Rev.*
601 *Biochem.* **80**, 587–612 (2011).

602 7. A. K. W. Elsholz, M. S. Birk, E. Charpentier, K. Turgay, Functional diversity of AAA+ protease
603 complexes in Bacillus subtilis. *Front. Mol. Biosci.* **4** (2017), doi:10.3389/fmolb.2017.00044.

604 8. E. Krüger, E. Witt, S. Ohlmeier, R. Hanschke, M. Hecker, The clp proteases of Bacillus subtilis are
605 directly involved in degradation of misfolded proteins. *J Bacteriol*. **182**, 3259–65 (2000).

606 9. I. Hantke, H. Schäfer, A. Janczikowski, K. Turgay, YocM a small heat shock protein can protect
607 Bacillus subtilis cells during salt stress. *Mol. Microbiol.* **111**, 423–440 (2019).

608 10. E. Krüger, U. Völker, M. Hecker, Stress induction of clpC in Bacillus subtilis and its involvement in
609 stress tolerance. *J Bacteriol*. **176**, 3360–3367 (1994).

610 11. T. Msadek, F. Kunst, G. Rapoport, MecB of Bacillus subtilis, a member of the ClpC ATPase family,
611 is a pleiotropic regulator controlling competence gene expression and growth at high
612 temperature. *Proc Natl Acad Sci U A*. **91**, 5788–92 (1994).

613 12. M. Persuh, I. Mandic-Mulec, D. Dubnau, A MecA paralog, YpbH, binds ClpC, affecting both
614 competence and sporulation. *J Bacteriol*. **184**, 2310–3. (2002).

615 13. T. Schlothauer, A. Mogk, D. A. Dougan, B. Bukau, K. Turgay, MecA, an adaptor protein necessary
616 for ClpC chaperone activity. *Proc. Natl. Acad. Sci. U. S. A.* **100**, 2306–2311 (2003).

617 14. K. Turgay, J. Hahn, J. Burghoorn, D. Dubnau, Competence in Bacillus subtilis is controlled by
618 regulated proteolysis of a transcription factor. *EMBO J.* **17**, 6730–6738 (1998).

619 15. J. Kirstein, D. A. Dougan, U. Gerth, M. Hecker, K. Turgay, The tyrosine kinase McsB is a regulated
620 adaptor protein for ClpCP. *EMBO J.* **26**, 2061–2070 (2007).

621 16. J. Fuhrmann, A. Schmidt, S. Spiess, A. Lehner, K. Turgay, K. Mechtler, E. Charpentier, T. Clausen,
622 McsB is a protein arginine kinase that phosphorylates and inhibits the heat-shock regulator
623 CtsR. *Science*. **324**, 1323–7 (2009).

624 17. A. K. W. Elsholz, K. Turgay, S. Michalik, B. Hessling, K. Gronau, D. Oertel, U. Mäder, J. Bernhardt,
625 D. Becher, M. Hecker, U. Gerth, Global impact of protein arginine phosphorylation on the
626 physiology of Bacillus subtilis. *Proc. Natl. Acad. Sci. U. S. A.* **109**, 7451–7456 (2012).

627 18. J. Fuhrmann, B. Mierzwa, D. B. Trentini, S. Spiess, A. Lehner, E. Charpentier, T. Clausen, Structural
628 basis for recognizing phosphoarginine and evolving residue-specific protein phosphatases in
629 gram-positive bacteria. *Cell Rep.* **3**, 1832–1839 (2013).

630 19. J. Kirstein, D. Zuhlke, U. Gerth, K. Turgay, M. Hecker, A tyrosine kinase and its activator control
631 the activity of the CtsR heat shock repressor in B. subtilis. *EMBO J*. **24**, 3435–45 (2005).

632 20. A. Schmidt, D. B. Trentini, S. Spiess, J. Fuhrmann, G. Ammerer, K. Mechtler, T. Clausen,
633 Quantitative phosphoproteomics reveals the role of protein arginine phosphorylation in the
634 bacterial stress response. *Mol. Cell. Proteomics MCP*. **13**, 537–550 (2014).

635 21. M. J. Suskiewicz, B. Hajdusits, R. Beveridge, A. Heuck, L. D. Vu, R. Kurzbauer, K. Hauer, V. Thoeny,
636 K. Rumpel, K. Mechtler, A. Meinhart, T. Clausen, Structure of McsB, a protein kinase for
637 regulated arginine phosphorylation. *Nat. Chem. Biol.* **15**, 510–518 (2019).

638 22. D. B. Trentini, M. J. Suskiewicz, A. Heuck, R. Kurzbauer, L. Deszcz, K. Mechtler, T. Clausen,
639 Arginine phosphorylation marks proteins for degradation by a Clp protease. *Nature*. **539**, 48–53
640 (2016).

641 23. A. K. W. Elsholz, S. Michalik, D. Zühlke, M. Hecker, U. Gerth, CtsR, the Gram-positive master
642 regulator of protein quality control, feels the heat. *EMBO J.* **29**, 3621–3629 (2010).

643 24. L. Stannek, K. Gunka, R. A. Care, U. Gerth, F. M. Commichau, Factors that mediate and prevent
644 degradation of the inactive and unstable GudB protein in Bacillus subtilis. *Front. Microbiol.* **5**,
645 758 (2014).

646 25. F. E. Morreale, S. Kleine, J. Leodolter, S. Junker, D. M. Hoi, S. Ovchinnikov, A. Okun, J. Kley, R.
647 Kurzbauer, L. Junk, S. Guha, D. Podlesainski, U. Kazmaier, G. Boehmelt, H. Weinstabl, K. Rumpel,
648 V. M. Schmiedel, M. Hartl, D. Haselbach, A. Meinhart, M. Kaiser, T. Clausen, BacPROTACs
649 mediate targeted protein degradation in bacteria. *Cell*. **185**, 2338-2353.e18 (2022).

650 26. B. Zhou, M. Semanjski, N. Orlovetskie, S. Bhattacharya, S. Alon, L. Argaman, N. Jarrous, Y. Zhang,
651 B. Macek, L. Sinai, S. Ben-Yehuda, Arginine dephosphorylation propels spore germination in
652 bacteria. *Proc. Natl. Acad. Sci. U. S. A.* **116**, 14228–14237 (2019).

653 27. B. Zhou, S. Alon, L. Rao, L. Sinai, S. Ben-Yehuda, Reviving the view: evidence that macromolecule
654 synthesis fuels bacterial spore germination. *microLife*. **3**, uqac004 (2022).

655 28. J. Kirstein, H. Strahl, N. Moliere, L. W. Hamoen, K. Turgay, Localization of general and regulatory
656 proteolysis in Bacillus subtilis cells. *Mol Microbiol*. **70**, 682–94 (2008).

657 29. P. Goloubinoff, A. Mogk, A. P. Zvi, T. Tomoyasu, B. Bukau, Sequential mechanism of solubilization
658 and refolding of stable protein aggregates by a bichaperone network. *Proc Natl Acad Sci U A*.
659 **96**, 13732–7 (1999).

660 30. T. Haslberger, A. Zdanowicz, I. Brand, J. Kirstein, K. Turgay, A. Mogk, B. Bukau, Protein
661 disaggregation by the AAA+ chaperone ClpB involves partial threading of looped polypeptide
662 segments. *Nat Struct Mol Biol*. **15**, 641–50 (2008).

663 31. J. Fuhrmann, V. Subramanian, P. R. Thompson, Synthesis and Use of a Phosphonate Amidine to
664 Generate an Anti-Phosphoarginine-Specific Antibody. *Angew. Chem. Int. Ed Engl.* **54**, 14715–
665 14718 (2015).

666 32. B. Hajdusits, M. J. Suskiewicz, N. Hundt, A. Meinhart, R. Kurzbauer, J. Leodolter, P. Kukura, T.
667 Clausen, McsB forms a gated kinase chamber to mark aberrant bacterial proteins for
668 degradation. *eLife*. **10**, e63505 (2021).

669 33. U. Gerth, J. Kirstein, J. Mostertz, T. Waldminghaus, M. Miethke, H. Kock, M. Hecker, Fine-tuning
670 in regulation of Clp protein content in Bacillus subtilis. *J. Bacteriol.* **186**, 179–191 (2004).

671 34. J. Muntel, V. Fromion, A. Goelzer, S. Maaβ, U. Mäder, K. Büttner, M. Hecker, D. Becher,
672 Comprehensive absolute quantification of the cytosolic proteome of Bacillus subtilis by data
673 independent, parallel fragmentation in liquid chromatography/mass spectrometry (LC/MS(E)).
674 *Mol. Cell. Proteomics MCP*. **13**, 1008–1019 (2014).

675 35. M. Babst, B. Wendland, E. J. Estepa, S. D. Emr, The Vps4p AAA ATPase regulates membrane
676 association of a Vps protein complex required for normal endosome function. *EMBO J*. **17**,
677 2982–93 (1998).

678 36. J. Kirstein, T. Schlothauer, D. A. Dougan, H. Lilie, G. Tischendorf, A. Mogk, B. Bukau, K. Turgay,
679 Adaptor protein controlled oligomerization activates the AAA+ protein ClpC. *EMBO J.* **25**, 1481–
680 1491 (2006).

681 37. J. Weibezahn, C. Schlieker, B. Bukau, A. Mogk, Characterization of a trap mutant of the AAA+
682 chaperone ClpB. *J Biol Chem*. **278**, 32608–32617 (2003).

683 38. Y. Ye, H. H. Meyer, T. A. Rapoport, The AAA ATPase Cdc48/p97 and its partners transport
684 proteins from the ER into the cytosol. *Nature*. **414**, 652–6 (2001).

685 39. A. J. Amor, K. R. Schmitz, T. A. Baker, R. T. Sauer, Roles of the ClpX IGF loops in ClpP association,
686 dissociation, and protein degradation. *Protein Sci. Publ. Protein Soc.* **28**, 756–765 (2019).

687 40. Y. I. Kim, I. Levchenko, K. Fraczkowska, R. V. Woodruff, R. T. Sauer, T. A. Baker, Molecular
688 determinants of complex formation between Clp/Hsp100 ATPases and the ClpP peptidase. *Nat*
689 *Struct Biol*. **8**, 230-233. (2001).

690 41. A. Martin, T. A. Baker, R. T. Sauer, Distinct static and dynamic interactions control ATPase-
691 peptidase communication in a AAA+ protease. *Mol Cell*. **27**, 41–52 (2007).

692 42. A. Tryggvesson, F. M. Ståhlberg, A. Mogk, K. Zeth, A. K. Clarke, Interaction specificity between
693 the chaperone and proteolytic components of the cyanobacterial Clp protease. *Biochem. J.* **446**,
694 311–320 (2012).

695 43. J. Weibezahn, P. Tessarz, C. Schlieker, R. Zahn, Z. Maglica, S. Lee, H. Zentgraf, E. U. Weber-Ban, D.
696 A. Dougan, F. T. F. Tsai, A. Mogk, B. Bukau, Thermotolerance requires refolding of aggregated
697 proteins by substrate translocation through the central pore of ClpB. *Cell*. **119**, 653–665 (2004).

698 44. C. Gatsogiannis, D. Balogh, F. Merino, S. Sieber, S. Raunser, Cryo-EM structure of the ClpXP
699 protein degradation machinery. *Nat. Struct. Mol. Biol.* **26**, 946–954 (2019).

700 45. B. G. Lee, E. Y. Park, K. E. Lee, H. Jeon, K. H. Sung, H. Paulsen, H. Rubsamen-Schaeff, H. Brotz-
701 Oesterhelt, H. K. Song, Structures of ClpP in complex with acyldepsipeptide antibiotics reveal its
702 activation mechanism. *Nat Struct Mol Biol*. **17**, 471–8 (2010).

703 46. J. Winkler, J. Tyedmers, B. Bukau, A. Mogk, Hsp70 targets Hsp100 chaperones to substrates for
704 protein disaggregation and prion fragmentation. *J. Cell Biol.* **198**, 387–404 (2012).

705 47. C. B. Anfinsen, Principles that Govern the Folding of Protein Chains. *Science*. **181**, 223–230
706 (1973).

707 48. W. E. Teague, G. P. Dobson, Thermodynamics of the arginine kinase reaction. *J. Biol. Chem.* **274**,
708 22459–22463 (1999).

709 49. N. B. Nillegoda, A. S. Wentink, B. Bukau, Protein Disaggregation in Multicellular Organisms.
710 *Trends Biochem. Sci.* **43**, 285–300 (2018).

711 50. C. Lee, K. B. Franke, S. M. Kamal, H. Kim, H. Lünsdorf, J. Jäger, M. Nimtz, J. Trček, L. Jänsch, B.
712 Bukau, A. Mogk, U. Römling, Stand-alone ClpG disaggregase confers superior heat tolerance to
713 bacteria. *Proc. Natl. Acad. Sci.* **115**, E273–E282 (2018).

714 51. P. Beltrao, P. Bork, N. J. Krogan, V. van Noort, Evolution and functional cross-talk of protein post-
715 translational modifications. *Mol. Syst. Biol.* **9**, 714 (2013).

716 52. I. Mijakovic, C. Grangeasse, K. Turgay, Exploring the diversity of protein modifications: special
717 bacterial phosphorylation systems. *FEMS Microbiol. Rev.* **40**, 398–417 (2016).

718 53. L. Ellgaard, A. Helenius, Quality control in the endoplasmic reticulum. *Nat Rev Mol Cell Biol*. **4**,
719 181–91 (2003).

720 54. M. H. Smith, H. L. Ploegh, J. S. Weissman, Road to ruin: targeting proteins for degradation in the
721 endoplasmic reticulum. *Science*. **334**, 1086–1090 (2011).

722 55. P. Walter, D. Ron, The unfolded protein response: from stress pathway to homeostatic
723 regulation. *Science*. **334**, 1081–1086 (2011).

724 56. E. Perrody, L. Abrami, M. Feldman, B. Kunz, S. Urbé, F. G. van der Goot, Ubiquitin-dependent
725 folding of the Wnt signaling coreceptor LRP6. *eLife*. **5** (2016), doi:10.7554/eLife.19083.

726 57. J. Sambrook, D. W. Russell, *Molecular cloning: a laboratory manual* (Cold Spring Harbor
727 Laboratory Press, Cold Spring Harbor, N.Y, 3rd ed., 2001).

728 58. C. Anagnostopoulos, J. Spizizen, REQUIREMENTS FOR TRANSFORMATION IN BACILLUS SUBTILIS.
729 *J. Bacteriol.* **81**, 741–746 (1961).

730 59. S. Runde, N. Molière, A. Heinz, E. Maisonneuve, A. Janczikowski, A. K. W. Elsholz, U. Gerth, M.
731 Hecker, K. Turgay, The role of thiol oxidative stress response in heat-induced protein aggregate
732 formation during thermotolerance in Bacillus subtilis. *Mol. Microbiol.* **91**, 1036–1052 (2014).

733 60. C. A. Schneider, W. S. Rasband, K. W. Eliceiri, NIH Image to ImageJ: 25 years of image analysis.
734 *Nat. Methods*. **9**, 671–675 (2012).

735 61. R. Lill, W. Dowhan, W. Wickner, The ATPase activity of SecA is regulated by acidic phospholipids,
736 SecY, and the Leader and mature domains of precursor proteins. *Cell*. **60**, 271–280 (1990).

737 62. K. Turgay, L. W. Hamoen, G. Venema, D. Dubnau, Biochemical characterization of a molecular
738 switch involving the heat shock protein ClpC, which controls the activity of ComK, the
739 competence transcription factor of Bacillus subtilis. *Genes Dev*. **11**, 119–28. (1997).

740 63. J. Schindelin, I. Arganda-Carreras, E. Frise, V. Kaynig, M. Longair, T. Pietzsch, S. Preibisch, C.
741 Rueden, S. Saalfeld, B. Schmid, J.-Y. Tinevez, D. J. White, V. Hartenstein, K. Eliceiri, P. Tomancak,
742 A. Cardona, Fiji: an open-source platform for biological-image analysis. *Nat. Methods*. **9**, 676–
743 682 (2012).

744 64. S. J. Fleishman, A. Leaver-Fay, J. E. Corn, E.-M. Strauch, S. D. Khare, N. Koga, J. Ashworth, P.
745 Murphy, F. Richter, G. Lemmon, J. Meiler, D. Baker, RosettaScripts: A Scripting Language
746 Interface to the Rosetta Macromolecular Modeling Suite. *PLOS ONE*. **6**, e20161 (2011).

747 65. F. Khatib, S. Cooper, M. D. Tyka, K. Xu, I. Makedon, Z. Popović, D. Baker, F. Players, Algorithm
748 discovery by protein folding game players. *Proc. Natl. Acad. Sci.* (2011),
749 doi:10.1073/pnas.1115898108.

750